



ELSEVIER

Computers in Biology and Medicine 34 (2004) 407–425

Computers in Biology
and Medicine

www.elsevierhealth.com/locate/combiomed

Intelligent training system integrated in an echocardiography simulator

M. Weidenbach^{a,b,*}, S. Trochim^a, S. Kreutter^a, C. Richter^c, T. Berlage^a, G. Grunst^a

^a*Fraunhofer Institute for Applied Information Technology, Schloss Birlinghoven, D-53754 Sankt Augustin, Germany*

^b*Department of Pediatric Cardiology, Heart Center, University of Leipzig, Strümpellstr. 39, D-04289 Leipzig, Germany*

^c*Department of Pediatric Cardiology, University of Bonn, Adenauerallee 119, D-53113 Bonn, Germany*

Abstract

Computer simulators play an important role in medical education. We have extended our simulator EchoComJ with an intelligent training system (ITS) to support trainees adjusting echocardiographic standard views. EchoComJ is an augmented reality application that combines real three-dimensional ultrasound data with a virtual heart model enabling one to simulate an echocardiographic examination. The ITS analyzes the image planes according to their position, orientation and the visualization of anatomical landmarks using fuzzy rules. An adaptive feedback is provided that colors the specific anatomic landmarks within the contours of the virtual model based on the quality of the image plane.

© 2003 Elsevier Ltd. All rights reserved.

Keywords: Education; Echocardiography; Cardiology; Simulation; Augmented reality; Artificial intelligence

1. Introduction

Echocardiography not only requires an extensive knowledge in cardiology, but also of sensorimotor (steering of the ultrasound transducer) and visual perceptive skills (analysis and interpretation of the ultrasound image). While the medical knowledge in cardiology is quite effectively provided by textbooks, journals and lectures, the practical skills can only be achieved through hands-on training [1]. Traditionally, these skills are therefore provided by a medical teacher on the job or in specially designed courses. While training on the job is a well-established and effective method for the trainee,

* Corresponding author. Department of Pediatric Cardiology, Heart Center, University of Leipzig, Strümpellstr. 39, D-04289 Leipzig, Germany. Tel.: +49-341-8650; fax: +49-163-2493710.

E-mail address: michael.weidenbach@medizin.uni-leipzig.de (M. Weidenbach).

this one-on-one training is rather ineffective for a diagnostic procedure with a very widespread use. Courses are not integrated in the daily work but have to be planned well in advance and require travel, thereby increasing the amount of time and expenses that have to be invested.

The almost ubiquitous availability of computers and the Internet produced a great amount of medical education software—also in the field of echocardiography [2–5]. Modern training software for medical professionals can simulate the working environment of physicians by Virtual Reality (VR) techniques [6–8]. The concept of Augmented Reality (AR) combines virtual three-dimensional (3D) environments with real image data [9,10]. In AR applications, the learner is dealing and interacts with real medical images. The VR models on the other hand enhance the information content of the images. Simulators provide the ability to interact with the virtual world in a realistic manner [7,9,11,12]. However, most of them still lack a crucial factor. They do not provide a teacher who assesses the operations of the trainee and gives immediate feedback [13]. Educational software should provide measures to verify the trainee's skills and give some feedback about his learning progress. This is necessary to motivate the trainee and to analyze his strengths and weaknesses.

2. Requirements and previous work

Echocardiographic simulators should use real ultrasound images to train the necessary perceptive skills that are needed to analyze the images that often differ from the trainee's mental concept of heart images, especially when they are distorted by backscatter noise and artifacts. In the AR simulator for echocardiography (EchoCom2) designed at the Fraunhofer Institute, we have registered 3D echocardiographic data sets temporally and spatially with a 3D VR model of the heart [14,15]. The interface basically consists of two parts. The right side of the split screen is the so-called "reference scene". Here, an animated virtual transducer and scan plane visualizes the spatial relationship between the transducer, the scan plane and the heart. On the left side a two-dimensional (2D) echocardiographic image is shown calculated from a 3D echocardiographic data set based on the positional data of the virtual scan plane. The trainee thus gets a visual explanation of the position of the ultrasound plane in relation to the 3D structure of the heart and in relation to the transducer (Fig. 1). For further clarification, the corresponding contours of the virtual heart (derived from the cardiac structures intersected by the virtual scan plane) can be projected overlying the ultrasound image. An input device designed as a dummy transducer, placed on a dummy torso, trains the hand-eye coordination. Both are equipped with an electromagnetic position and orientation system, tracking the position of the virtual image plane in real time [16]. Thus, an echocardiographic examination can be simulated (Fig. 2). The technical details of the system are described in detail elsewhere [15]. Although in EchoCom2 there is a visual feedback to the trainee, his actions are not analyzed. There is the danger that wrong concepts will be internalized when not supervised. Even if the trainee has identified problems and incorrect image planes, frustrations may arise, if the problem cannot be solved. Ideally, the teacher should not simply give corrections but should support the trainee to find the correct solution (here the correct image) himself. The support should not be static but should meet the individual needs of each trainee. The solution for this problem can be training systems based on artificial intelligence (AI) techniques that observe and analyze the learner's behavior and give appropriate support [17].

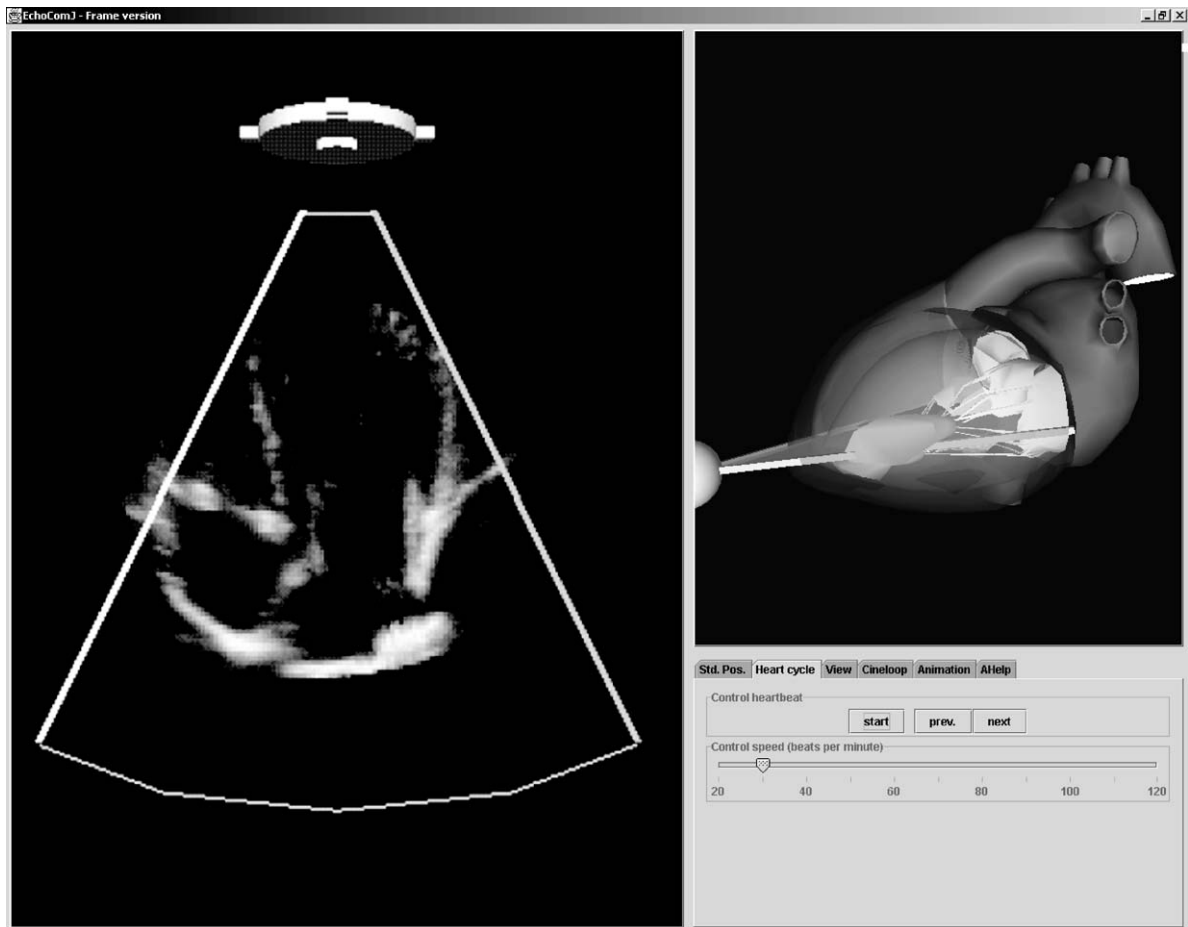


Fig. 1. Interface of the AR simulator EchoComJ. The reference scene on the right side of the screen demonstrates the spatial relationship between the image plane and the heart. Based on the coordinates of this image plane, the echocardiographic image on the left side is calculated from a registered 3D ultrasound data set. Below the reference scene is a control panel for various modifications of the scene, e.g. to control the speed of the animated heartbeat.

3. Methods

3.1. Analysis of standard views

The goal of our integrated intelligent training system (ITS) was to support beginners adjusting echocardiographic standard views. For the acquisition of 3D echocardiographic data sets, we used a Vingmed System V scanner (Vingmed Sound A/S, Horton, Norway) attached to a workstation with dedicated software for 3D reconstruction (4D EchoScan, TomTech GmbH, Munich, Germany) as described by Weidenbach et al. [15]. Since we have used 3D echocardiographic data sets depicting the complete heart, the data sets have been acquired by an apical or parasternal transthoracic approach. We have shown that not only normal but also pathologic data sets can be registered with the heart

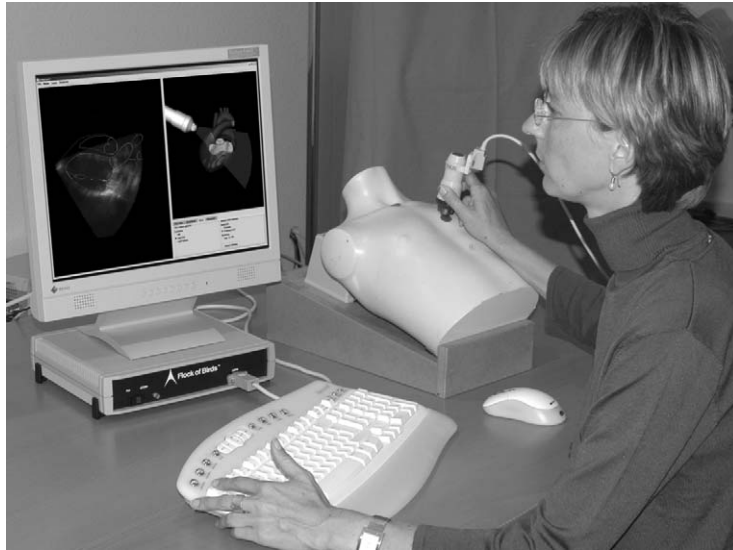


Fig. 2. Simulation of a 2D echocardiographic examination with a dummy transducer and a dummy torso equipped with a position sensor. This position sensor controls the image plane on the screen.

model [18]. However, certain anatomic structures, like the aortic arch, are not sufficiently visualized. We therefore concentrated on apical and parasternal standard views. In order to provide adaptive support, the ITS has to be able to judge the quality of the acquired ultrasound plane. Therefore, one needs a similarity measure indicating, which is the closest standard view and how well the current plane approaches the optimal plane regarding its position and orientation. One limitation is that a sole correct standard view cannot exactly be defined. For each view there is an indefinite number of minor variations of the optimal transducer position and orientation that yields good or at least acceptable images. These tolerance intervals have to be flexible and depend on the standard plane itself. Due to this natural fuzziness we chose an approach based on fuzzy sets [19]. Fuzzy sets are used to describe vague concepts. They can be understood as generalized normal (crisp) sets, where one element belongs to a set with a membership degree between 0 and 1. One element can belong to more than one class or set. The standard views are evaluated in a two-step classification scheme. At first, the position of the transducer head is validated. Only if the position is valid, the quality of the standard view is analyzed. For the representation of the transducer head position and the plane orientation we derived a fuzzy membership function for each head position and standard view respectively from a training data set. This training data set was acquired by an experienced sonographer who adjusted 10 times the parasternal and apical standard views including the transitions between them (Table 1).

3.2. Analysis of transducer position and orientation of the image plane

The representation of the transducer position and the orientation of a standard view are based on a fuzzy clustering of the training data set (see Appendix A). Positional data and normal vectors are clustered separately in order to get an independent representation of the transducer position

Table 1
Integrated standard views

Parasternal transducer position

Parasternal long axis left ventricle; landmarks: LV, MV, AoV
 Parasternal short axis aortic valve; landmarks: AoV, TV, PulV
 Parasternal short axis mitral valve; landmarks: MV
 Parasternal short axis midventricular; landmarks: PAP
 Parasternal bifurcation of main pulmonary artery

Apical transducer position

Apical four-chamber view; landmarks: LV, MV, TV
 Apical five-chamber view; landmarks: LV, MV, AoV
 Apical two-chamber view; landmarks: LV, MV,
 Apical long axis; landmarks: LV, MV, AoV

LV—left ventricle; MV—mitral valve; AoV—aortic valve; TV—tricuspid valve; PulV—pulmonary valve; PAP—papillary muscles.

and the orientation of the standard view in relation to the heart model. From the training data, three clusters for the parasternal transducer position (third, fourth and fifth intercostal space) and three clusters for the apical transducer position (valid, too far above, too far medial) were derived. The two concepts “too far medial” and “too far above” correspond to an incorrectly shortened visualization of the left ventricle. The cluster analysis of normal vectors yielded six clusters for the apical trajectories, four of which are relevant: apical four-chamber view, apical five-chamber view, apical two-chamber view, apical long axis left ventricle. For the parasternal transducer position there are five clusters: parasternal short axis aortic valve, parasternal short axis mitral valve, parasternal short axis left ventricle, parasternal long axis left ventricle, bifurcation of the pulmonary artery. From these calculated cluster prototypes we derived fuzzy membership functions as gaussians (see Appendix A). The distance between the transducer head position and the shell of the clusters along one vector represents the membership degree of the vector to the normal cluster (Fig. 3).

3.3. Analysis of anatomic landmarks

The anatomic landmarks for each standard view are described in the table. They comprise the heart valves, the papillary muscles and the apex of the left ventricle. Especially the heart valves change their position relative to the ultrasound plane during the heart cycle, whereas the ultrasound plane itself remains nearly constant. Therefore, a solution is needed accounting for the whole range of motion of the given heart structure. Because of their favorable geometric characteristics we chose circumscribing ellipsoids to represent the heart valves, which are determined from the wire-frame of the virtual heart model. The area of intersection of the image plane with the ellipsoid represents the quality of the visualization of the landmark (Fig. 4). For the left ventricle we used an inscribing ellipsoid. The relation between the maximal possible area of intersection and the measured area of intersection can be interpreted as a fuzzy membership function describing the validity of a specific landmark (see Appendix B) [20].

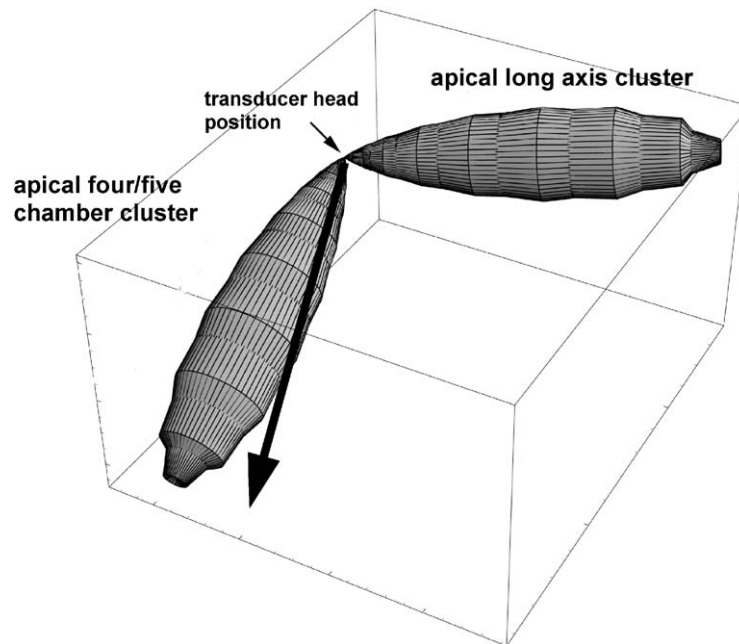


Fig. 3. Example of two apical standard view clusters. The bold arrow represents the normal vector of an arbitrary image plane. The membership value of this image plane to the cluster depends on the length of the vector within the shell of the cluster.

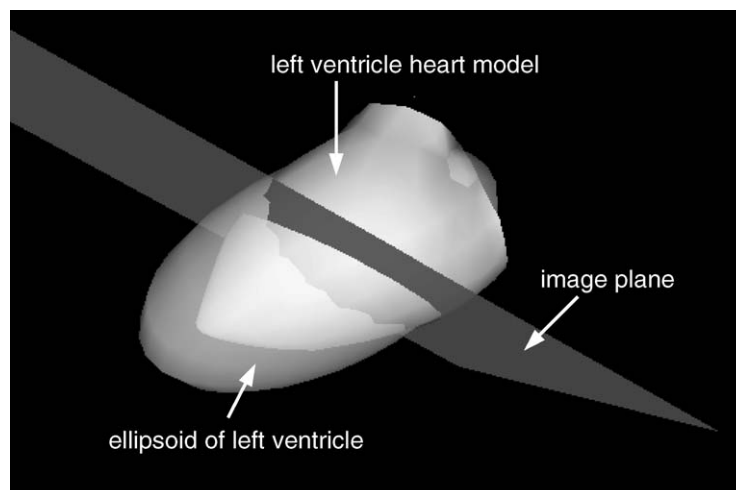


Fig. 4. Assessment of landmark visualization demonstrated for the landmark “left ventricle”. To simplify the calculations not the landmarks themselves are used for assessment but ellipsoids that represent these. The quality of the visualization improves with an increase in the area of intersection of the ellipsoid and the image plane.

3.4. Fuzzy rules

The two criteria orientation of the image plane and visibility of landmarks are combined by fuzzy rules [17]. Single membership values of the corresponding landmarks for each standard view are aggregated by a minimum function. This value is then aggregated with the membership value of the plane orientation (normal vector) as weighted average. Standstills are analyzed exclusively. A standstill is defined as no or just minimal motion within a time frame of 1 s.

The corresponding fuzzy rule, e.g. for the apical four-chamber view is defined as follows:

if	<i>[positionApical]</i>	and	<i>normal vector apical four-chamber view</i>	
	and	<i>RingMV</i>	and	<i>RingTV</i>
	and	<i>AreaLV</i>	and not	<i>RingAoV</i>
then	<i>apical four-chamber view</i>			

MV—mitral valve; TV—tricuspid valve; LV—left ventricle; AoV—aortic valve.

In this example of the apical four-chamber view the MV, the TV, and the LV have to be visualized within the plane, while the AoV must not. Positional data and landmark visualization are always assessed in relation to the heart model and not in relation to individual 3D echocardiographic data sets. However, since the 3D echocardiographic data sets are registered temporally and spatially with the heart model, these data are transferable to the ultrasound data. Still, it has to be taken into account that the registration never yields an absolute congruence between the model and the echocardiographic data sets.

3.5. Adaptive support

To avoid distraction from the ultrasound image any visual support for the trainee should be integrated into the scene. Therefore, we have designed an adaptive highlighting of the relevant landmarks for each standard view within the heart model contours. Based on the assumption that the learner is trying to adjust the standard view closest to the actual plane, the appropriate landmarks for highlighting are automatically selected. That means, e.g. for the apical four-chamber view the MV, TV and LV are highlighted, while in the apical five-chamber view the appropriate landmarks are the MV, AoV and LV (see table). To give the trainee immediate feedback on how well the desired standard view is adjusted, all relevant structures are highlighted and colored depending on the quality of adjustment. Red indicates a poor, yellow a medium and green a good adjustment. Thus, different coloring of each of the relevant structures indicates the resulting quality of the actual image plane. When all structures show green, this indicates an optimal standard view (Fig. 5).

4. Implementation

The Echocardiographic Training Simulator was implemented in the Java programming language using Java3D as its 3D graphics library. This way the system does not rely on a specific hardware or software platform and is able to run on different operating systems (Windows NT/2000/XP, Linux and Solaris). On top of the Java environment a generic framework for medical 3D image

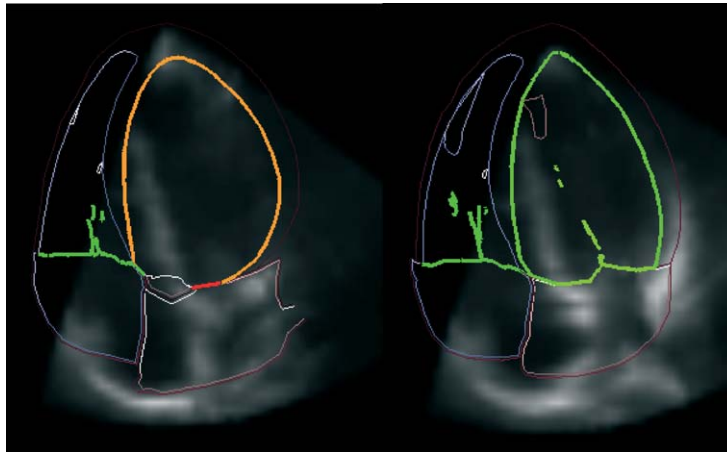


Fig. 5. According to the quality of the image plane the contours of the landmarks are colored. In the left image the LV is sub optimally visualized, the mitral valve poorly and the tricuspid valve well. After accurate adjustment of the image plane all landmarks are colored green indicating a perfect apical four-chamber view. Note that the contours of the heart model and the ultrasound image are not absolutely congruent due to the inherent inaccuracy of the registration of individual 3D ultrasound data sets to a non-deformable heart model.



Fig. 7. Example of a “near standard plane”. The image is not an accurate standard view but is close enough to assume that the user intended to adjust a five-chamber view.

processing builds the basis of the training simulator. Three additional modules had to be developed and integrated: (a) a sensorimotor analysis component to monitor and interpret user interaction, (b) a component to give adaptive feedback according to the current context and (c) a movement recorder to allow re-evaluation and discussion of a simulated examination. Fig. 6 shows the system's

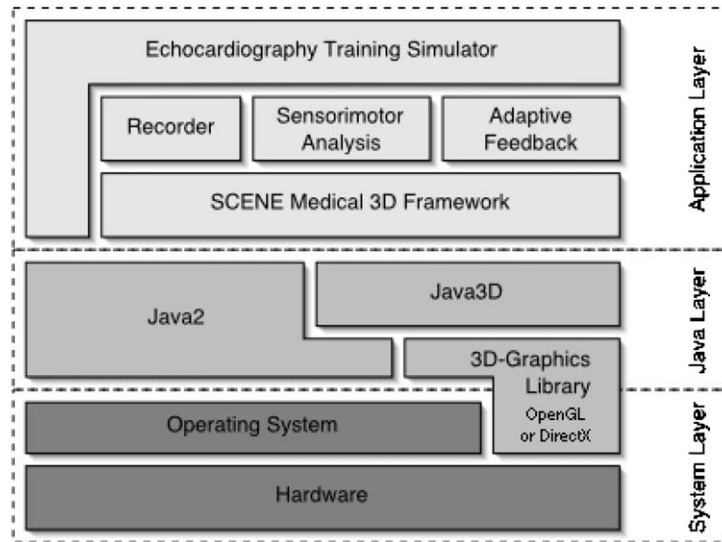


Fig. 6. Implementation of EchoComJ and the integrated ITS.

architecture and its different layers. The software counts more than 80,000 lines of code in about 350 classes and interfaces. The implementation of the 3D image processing framework took about 2 man years of development time and was a complete rewrite of a 3D ultrasound simulator written in C++/OpenInventor. Additional 2 man years were spent on developing the sensorimotor analysis and the adaptive feedback component. Most of this time was spent on evaluating several fuzzy-methods and clustering algorithms and fine-tuning their parameters. The Training Simulator runs smoothly on a 1GHz Pentium III with Nvidia GeForce2 and 384MB RAM or equivalent systems.

5. Evaluation

We have done a preliminary evaluation to verify the ability of the ITS to correctly classify image planes. As described in the chapter “fuzzy rules”, a membership value for the cluster of the corresponding standard view is calculated for every image plane. The value “one” is assigned if the image normal vector is equivalent to the normal vector of the cluster and the landmarks are optimally visualized, indicating a perfect standard view. The value “zero” on the other hand is assigned to an image normal vector without relation to the cluster and if there is no intersection of the image plane with the respective landmarks. Based on the assigned value image planes are classified as “standard view”, “near standard view” or “no standard view”. The category “near standard view” is assigned to image planes that do not fulfill the criteria of standard views but allow to assume the user intended to adjust the respective standard view (Fig. 7). A membership range of 0.6–1 defines an image as “standard view”, the range between 0.3 and 0.6 as “near standard view” and below 0.3 as “no standard view”. In a first step, image planes were adjusted using the ITS. Guided by the coloring of the heart contours and the membership value for the clusters a total of 110 “standard views”, 30 “near standard views” and 16 “no standard views” were adjusted. All images classified

as “no standard view” had a membership value greater than 0 to prevent analyzing images that were too obviously invalid. The images were then stored, blinded and presented to two experienced sonographers. One of the sonographers was familiar with the system while the other one was not. Both classified the images into the same categories as the system. At first, the sonographers assessed the adjusted image planes considering only the heart model contours. Afterwards, these contours were removed and the plane of the underlying ultrasound image was assessed. Whether contours are shown or not, it should be remembered that the positional data and the landmark visualization are assessed in regard to the heart model and not to individual 3D echocardiographic data sets. The results are shown in Fig. 8a. Since there were only marginal differences between the classifications of the two sonographers they are grouped together. There was an agreement between the ITS and the sonographers of 85% for the class “standard view”, while 13% of the views classified by the ITS as “standard view” were classified as “near standard view” by the sonographers. Only 3% were classified as “no standard view” by the sonographers. The results for those views classified by the system as “near standard view” or “no standard view” respectively were similar (Fig. 8a). For the assessment of the ultrasound images, only “standard views” were evaluated because of the reduced quality of the ultrasound data sets and the difficulty to identify views when too few landmarks were visualized. As expected, the accordance of these images was less compared to the images of the heart contours. In a second approach, the experienced sonographers adjusted image planes without interference of the training module. The image planes were then classified by the system to check, if the system would identify these images correctly. The sonographers adjusted 32 “standard views” and 16 “no standard views” considering the heart model contours and 12 “standard views” considering the ultrasound images. Again there was a high degree of accordance between the ITS and the sonographers with better results for the images of the heart contours (Fig. 8b).

6. Discussion

Simulators can effectively impart clinical skills [21,22] and medical procedures [11]. Simulators are an integrated part of the curriculum of medical schools [23] and their use is recommended by the American College of Cardiology Task Force on Education [24]. Currently, an increasing number of training simulators have been developed, some of them generating a very realistic scene into which the trainee can immerse himself [12,13]. In echocardiography, the development of necessary sensorimotor and perceptive skills by traditional static learning media is sub-optimal. These skills can only be properly transmitted via a hands-on-training. Since echocardiographic images often do not meet the learner’s expectation patterns in regard to the 3D anatomy of the heart we have enriched the echocardiographic images with a virtual 3D scene. This VR scene visualizes the most important anatomical structures and demonstrates the spatial relationship of these structures to the ultrasound probe and the corresponding image plane. This concept of integrating “real” and virtual images is an essential part of AR applications [10] and was realized in EchoCom2. During testing in clinical routine it became clear that the simulator could not fulfill the expectations without supervision of an experienced sonographer. However, it was exactly this human teacher that we at least partially wanted to substitute. To provide the trainee with appropriate help and motivation we had to integrate the function of such a “trainer” into the system. AI methods are used when the computer addresses individual needs in human–computer interaction. The design of the presented system is similar to

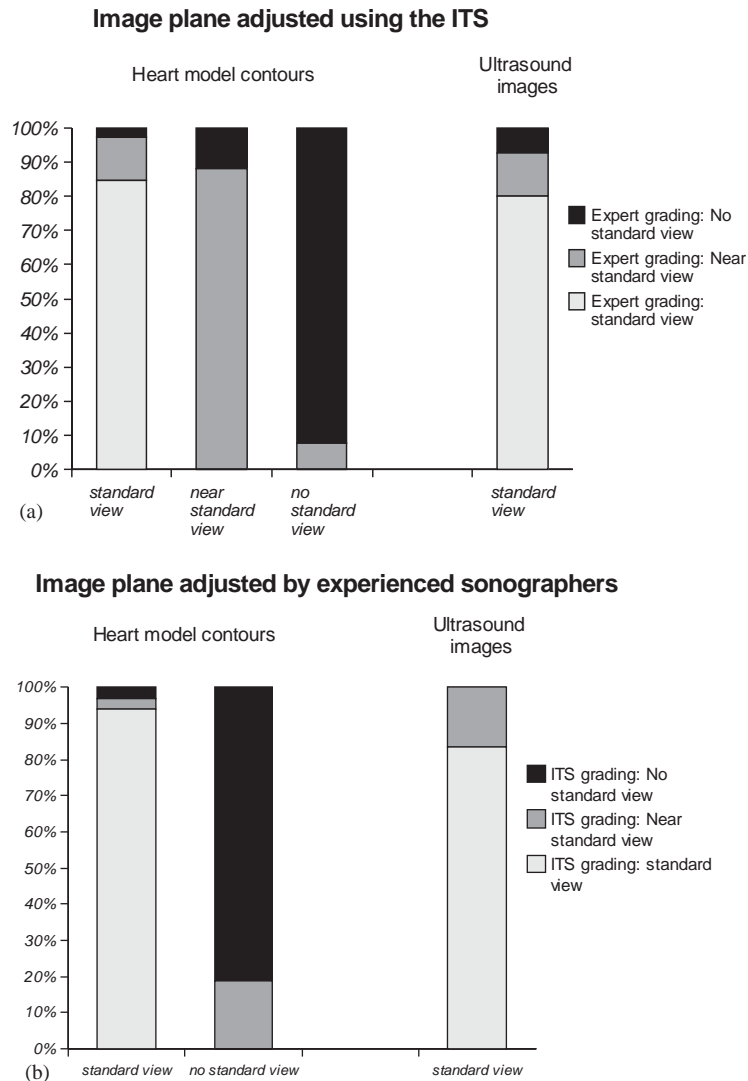


Fig. 8. (a) Each bar represents one image category adjusted using the guidance of the ITS. The different colors represent the classification of these images by the sonographers. In the left three bars the contours of the heart model, while in the right bar the ultrasound images derived from the 3D data sets were assessed by the sonographers. (b) Each bar represents one image category adjusted by the sonographers. The different colors represent the classification of these images by the ITS. In the two bars on the left the contours of the heart model, while in the right bar the ultrasound images derived from the 3D data sets were assessed by the ITS.

the echocardiography simulator EchoCom2. However, an AI component is integrated to analyze the user's actions and to support him in his learning process. The application is implemented as a Java-applet to be independent of the operating system and for future use via the Internet. In the beginning the trainee has to understand the 3D anatomy of the heart and its relation to tomographic views obtained by echocardiography. In our system this is achieved by free exploration of the heart

model and the registered 3D ultrasound data sets. The beginner, however, will soon get lost in this 3D space, since he has neither yet developed the necessary visual perceptive skills for orientation, nor the sensorimotor skills for navigation of the transducer to visualize the relevant structures of the heart. Besides their use in clinical routine, standard views provide the beginner with visual markers to detect the relevant anatomic structures. Since the system has AI capabilities similar to a trainer it therefore should support the correct adjustment of echocardiographic standard views. Since in our registered 3D echocardiographic data sets the supracardiac structures are not at all visualized or in such poor quality we focused on apical and parasternal standard views. Standard views in echocardiography are defined by orientation of the image plane resulting in visualization of specific anatomical landmarks providing a heart of normal anatomy [25]. The average echocardiographic examination is compromised by obesity, bony abnormalities, and superimposition of air or surgical scar tissue. Even if it were possible to define a perfect standard view based on the definition above, standard views in reality are nearly always a compromise between the defined image orientation and the patient's specific limitations. Even an experienced sonographer will not adjust an exact standard plane in the same patient with identical orientation in two consecutive examinations [26]. The transition of optimal standard views to sub-optimal or unacceptable views is fluent and is influenced by subjective judgment despite clear definitions. We have used a fuzzy set approach to define the membership degree of image planes to standard view clusters. Nevertheless, in preliminary tests, it became clear that defining standard views by transducer position and image orientation alone was insufficient in particular instances. A slight anterior angling of the transducer from the four-chamber view yields the five-chamber view with visualization of the left ventricular outflow tract and aortic valve. Since the beginner has to differentiate between these two important standard views, visualization of the aortic valve should be strictly avoided when adjusting the four-chamber view. However, the clusters of these two views demonstrated a substantial overlap. A similar problem was encountered in the parasternal short axis view adjusting the cross-section of the aortic valve. A slight tilt toward the apex resulted in an image plane below the aortic valve yielding an insufficient image plane. We therefore needed an additional distinguishing feature. We have chosen specific anatomic landmarks that have to be included or excluded to define the respective standard view. This information was combined with the vector data using fuzzy rules. Landmarks guide sonographers to a correct position of the image plane. The non-experienced sonographer tries to find the correct image plane by optimizing all relevant landmarks one by one. However, he is prone to lose optimal visualization of the current landmark once trying to adjust a subsequent one, since he is only able to concentrate on one object at a time. An experienced sonographer on the other hand does not adjust one landmark after another. Intuitive variation of the current plane combined with simultaneous consideration of all relevant landmarks until the image plane meets the expectation patterns of his mental engram leads the expert to the respective standard view. We have taken this intuitive approach into account when designing the adaptive support. A number of relevant landmarks for each standard view were defined. The contours of these specific landmarks were colored within the heart model contour overlay according to the quality of their visualization. We chose the colors of a traffic light to intuitively signal the current status of adjustment. This guarantees that the attention of the trainee is always focused on all relevant structures at a time. If the visualization of one landmark is worsened while adjusting another, a color shift from green to yellow or red promptly signals this. The trainee thus is taught to concentrate on the picture as a whole and not only on separate structures.

In a preliminary evaluation we tested, if the system can correctly assess views. There was a high degree of accordance between the assessment of the system and the assessment of two experienced sonographers. Also, the results for the registered ultrasound data sets were surprisingly good, taking into account that the ultrasound plane is highly dependent on the registration and the inherent mismatch of the ultrasound data and the heart model. In addition to the categories “standard view” and “no standard view”, we have defined an extra category “near standard view” for two reasons. First, it is motivating to the trainee to receive encouraging feedback when approaching a standard view. Second, it could be used by the ITS as a trigger for additional support. If the ITS detects for example that the trainee is not able to properly adjust a standard view after a certain time despite being close to it, appropriate instructions could be given. One possibility is to give commands such as “rotate left to improve visualization of the aortic valve”. Another option is to present the correct image plane together with the current view in the reference scenario. Our evaluation of course can only be a first step to a more thorough evaluation. The correct identification of images by the ITS, however, is a *sine qua non*. Future evaluations must demonstrate a benefit to echocardiographic training. May it be to achieve the training goal in a shorter time, to a higher level of expertise within a given time or with less expenses. So far we only focused on the final image frame of an echocardiographic sweep, namely the standard view. However, it is of equal importance how this endpoint is reached. Has it been reached directly or have there been moments of disorientation, how long was the elapsing time, etc. It is important for an adaptive training system to analyze transitions between two views. Interference may be necessary when the trainee is at risk of getting lost. Uncontrolled sweeps have to be separated from intended sweeps to visualize a certain region as well as transitions between two intended views. Identification of these different types of movement are important discriminators to trigger specific help modules. Preliminary steps towards this discrimination using Hidden Markov Models showed promising results [27]. Currently, the system is a prototype. The aim is to integrate it into a fully computerized echocardiographic course as well as into the curriculum. With certain alterations use via the Internet is possible. The training of non-cardiologists in remote sites would for example be an interesting plan for the future.

7. Summary

EchoComJ is an AR application that enables its user to simulate a 2D echocardiographic examination. Positional and orientation data of a dummy transducer are tracked by an electromagnetic position and orientation system to navigate a virtual scan plane. Tomographic images derived from 3D echocardiographic data sets are represented side-by-side with a 3D virtual heart model to illustrate the spatial relationship between heart, scan plane and resulting echocardiographic image. An ITS is integrated to partly substitute the human teacher. The implemented ITS focuses on imparting the adjustment of apical and parasternal echocardiographic standard views which are extremely important to the beginner for orientation. However, a sole correct standard view cannot be defined, since for each standard view an indefinite number of minor variations exists. We chose an approach based on fuzzy sets to analyze the images taking into account the fluent transition between acceptable and non-acceptable image planes. Standard views were defined by position and orientation of the virtual image plane and by visualization of anatomic landmarks. The representation of the transducer position and the orientation of a standard view is based on a fuzzy clustering of a training data set that

was generated by a sonographer adjusting the respective standard views. The cluster analysis of the normal vectors yielded cluster prototypes from which fuzzy membership functions for random image planes were derived. The anatomic landmarks comprise the heart valves and the left ventricle of the virtual heart model. To analyze the quality of landmark visualization not the landmarks themselves are considered, but their representation by ellipsoids. The area of intersection between the image plane and the respective ellipsoid defines the quality of visualization. This information and the orientation data are combined using fuzzy rules. According to the membership value the images were defined as “standard view”, “near standard view” or “no standard view”. In a preliminary evaluation we could demonstrate that the assessment of the ITS in regard to these three categories was similar to the assessment of two experienced sonographers. To teach the trainee the adjustment of standard views we have designed an adaptive support. Based on the quality of landmark visualization, the tomographic contours of the heart model that are optionally superimposed on the ultrasound images are colored. The colors green, yellow or red intuitively indicate a good, medium or poor result respectively. Each landmark is colored separately to point out which of the structures are visualized and have to be adjusted to receive the respective standard view. However, since all relevant structures are colored simultaneously, the attention of the trainee is always focused on the whole image and not on single structures. It enables him to intuitively adjust echocardiographic standard views guided by the ITS. The Echocardiographic Training Simulator was implemented in the Java programming language and thus is independent of a specific hardware or software platform and is able to run on different operating systems.

Appendix A. Fuzzy clustering of transducer head positions and normal vectors

The representation of the transducer position and the orientation of a standard view is based on a fuzzy clustering of the training data. Position and normal vectors are clustered separately in order to get an independent representation of the transducer position and the orientation of the standard view in relation to the heart model. In a two-step classification scheme the position is analyzed first and only if it is valid the standard view is classified.

A.1. Clustering of position vectors

The position vectors are clustered using the fuzzy c-means algorithm [26]. It aims at finding a suitable fuzzy partition for a given data set $X = \{x_1, \dots, x_n\} \subseteq \mathcal{R}^p$, where each datum is assigned to each class or cluster with a membership degree between zero and one. Most clustering algorithms aim at calculating a suitable prototype v_i for each cluster i and a membership degree $u_{ik} = u_i(x_k) \in [0, 1]$ for each datum $x_k \in X$, given a fixed number of clusters c . This can be done by minimizing the following objective function:

$$J(X, U, V) = \sum_{i=1}^c \sum_{k=1}^n (u_{ik})^m d^2(v_i, x_k), \quad (\text{A.1})$$

under the following constraints:

$$\sum_{k=1}^n u_{ik} > 0 \quad \text{for all } i \in \{1, \dots, c\} \quad (\text{A.2})$$

and

$$\sum_{i=1}^c u_{ik} = 1 \quad \text{for all } k \in \{1, \dots, n\}. \quad (\text{A.3})$$

c is the number of clusters and $d(v_i, x_k)$ is the distance between prototype v_i and datum x_k . The parameter $m > 1$ is the so-called fuzziness index and is usually chosen as 2. For $m \rightarrow 1$ the clusters tend to be crisp, i.e. $u_{ik} \rightarrow 1$ or $u_{ik} \rightarrow 0$, for $m \rightarrow \infty$ we get $u_{ik} \rightarrow 1/c$.

The objective function (1) uses the sum of the weighted distances of the data to the clusters. (2) ensures that no cluster is empty and (3) guarantees that the sum of the membership degrees of one datum to all clusters is one.

By differentiating the Lagrange function of (1) taking into account (3) we get

$$u_{ik} = \frac{1}{\sum_{j=1}^c \left(\frac{d^2(v_i, x_k)}{d^2(v_j, x_k)} \right)^{1/(m-1)}} \quad (\text{A.4})$$

as a necessary condition for the membership degrees for a local minimum of (1), given the prototypes are fixed. Similarly, we can derive a necessary condition for the prototypes

$$v_i = \frac{\sum_{k=1}^n u_{ik}^m x_k}{\sum_{k=1}^n u_{ik}^m}. \quad (\text{A.5})$$

Starting with a random initialization for the prototypes and membership degrees and alternately applying (4) and (5), we can optimize the prototypes and membership degrees until the changes are smaller than a given threshold ε .

The simplest fuzzy clustering algorithm, the *fuzzy c-means*, uses the Euclidean distance for d . In this case the prototypes are p -dimensional vectors and the algorithm finds almost spherical clusters.

A.2. Clustering of normal vectors

After the transducer head position is chosen, the main difficulty consists of steering the probe by rotation and tilting, which is completely described by the normal vector of the ultrasound plane. For the cluster analysis we need an angle-based distance measure, which defines the distance between two vectors. Klawonn and Keller [28] proposed a variant of the fuzzy c-means algorithm, which takes the dot product of two vectors into account. The distance between a normalized vector x and a normalized prototype vector v is then defined as

$$d^2(v, x) = 1 - v^T x.$$

Thus, we have $0 \leq d^2(v, x) \leq 2$ and $d^2(v, x) = 0 \Leftrightarrow x = v$. Under the constraint that the prototype vectors have to be normalized, i.e.

$$\|v_i\|^2 = \sum_{t=1}^p v_{it}^2 = 1$$

we can build the partial derivatives of a corresponding Lagrange function of (1), using the new distance measure, yielding

$$v_{il} = \frac{\sum_{k=1}^n u_{ik}^m x_{kl}}{\sqrt{\sum_{t=1}^p (\sum_{k=1}^n u_{ik}^m x_{kt})^2}}$$

as the new updating rule for the prototypes.

A.3. Derivation of fuzzy membership functions

For each cluster prototype we derived a fuzzy membership function representing the corresponding standard plane and transducer head position respectively. We chose an approximate solution representing each cluster by a Gaussian. The common membership function for cluster i is then

$$\mu_i(x) = e^{-a(d^2(v_i, x)/\sigma_i^2)},$$

where σ_i^2 represents the fuzzy estimate of the mean distance of all data to the prototype v_i

$$\sigma_i^2 = \frac{\sum_{k=1}^n u_{ik}^m d^2(v_i, x_k)}{\sum_{k=1}^n u_{ik}^m}.$$

The factor a is chosen to guarantee a fixed membership value α for $d^2(v_i, x_k) = \sigma^2$. Thus, a is set as $a = -\ln \alpha$. Usually $\alpha = 0.75$ was chosen.

Appendix B. Analysis of anatomic landmarks

We have chosen inscribing or circumscribing ellipsoids respectively to represent the landmarks because of their favorable geometric characteristics. This allows an easy and fast calculation of the quality of adjustment.

Orientation, size and position are derived from the landmark vertices of the heart's wireframe model [15]. We used a singular value decomposition of the central moment matrix computed from the vertices of a relevant heart structure. The matrix A of central moments of all vertices moments of all vertices $P_i = (x_i, y_i, z_i)$ with the centroid $C = (\bar{x}, \bar{y}, \bar{z})$ is defined as

$$A = \begin{bmatrix} \sum_{i=1}^n (x_i - \bar{x})(x_i - \bar{x}) & \sum_{i=1}^n (x_i - \bar{x})(y_i - \bar{y}) & \sum_{i=1}^n (x_i - \bar{x})(z_i - \bar{z}) \\ \sum_{i=1}^n (y_i - \bar{y})(x_i - \bar{x}) & \sum_{i=1}^n (y_i - \bar{y})(y_i - \bar{y}) & \sum_{i=1}^n (y_i - \bar{y})(z_i - \bar{z}) \\ \sum_{i=1}^n (z_i - \bar{z})(x_i - \bar{x}) & \sum_{i=1}^n (z_i - \bar{z})(y_i - \bar{y}) & \sum_{i=1}^n (z_i - \bar{z})(z_i - \bar{z}) \end{bmatrix},$$

$$C = \frac{1}{n} \begin{pmatrix} \sum_{i=1}^n x_i \\ \sum_{i=1}^n y_i \\ \sum_{i=1}^n z_i \end{pmatrix}.$$

Using the singular value decomposition we can decompose A to its eigenvectors and eigenvalues:

$$A = U \cdot S \cdot V',$$

where U is the matrix of the eigenvectors and S is the diagonal matrix of the eigenvalues.

$$U = \begin{bmatrix} e_{1_x} & e_{2_x} & e_{3_x} \\ e_{1_y} & e_{2_y} & e_{3_y} \\ e_{1_z} & e_{2_z} & e_{3_z} \end{bmatrix}, \quad S = \begin{bmatrix} \sigma_1 & & \\ & \sigma_2 & \\ & & \sigma_3 \end{bmatrix}, \quad \sigma_1 \geq \sigma_2 \geq \sigma_3.$$

The eigenvectors define the direction of the “main axes” of the vertex set with their lengths defined by the eigenvalues. The ellipsoid axes are defined by the eigenvectors e_1, e_2 and e_3 with a scaled and normalized length of:

$$a = \frac{1}{2}\sqrt{\sigma_1}, \quad b = \frac{1}{2}\sqrt{\sigma_2}, \quad c = \frac{1}{2}\sqrt{\sigma_3},$$

$$\text{ellipsoid} := \frac{x^2}{a^2} + \frac{y^2}{b^2} + \frac{z^2}{c^2} - 1 = 0.$$

The quality of landmark visualization is defined by the quotient of the current slice plane area and the maximum slice plane area:

$$q_{\text{ellipsoid}} = \frac{A_{\text{intersection}}}{\pi \max_1(a, b, c) \max_2(a, b, c)}, \quad 0 \leq q_{\text{ellipsoid}} \leq 1,$$

where the function $\max_n(a, b, c)$ selects the n th maximum of its arguments. The area is computed by approximation. First, a sufficient number of points on the intersection curve are computed to get a polygon that closely matches the ellipsoid. The area of this polygon can be computed by

$$A_{\text{polygon}} = \left| \frac{1}{2} \sum_{i=1}^{n-1} (x_i - x_{i+1})(y_i - y_{i+1}) \right| = \left| \frac{1}{2} \sum_{i=1}^{n-1} (x_i y_{i+1} - x_{i+1} y_i) \right|.$$

If a heart valve defines the landmark and the image plane is perpendicular to the valve only the ring of the valve has to be considered. The quality is then defined by the distance of the intersections

points p and q with an ellipse (describing the valve) and the ultrasound plane:

$$q_{\text{ellipse}} = \frac{d(p, q)}{2 \max(a, b)}, \quad 0 \leq q_{\text{ellipse}} \leq 1,$$

$$d(p, q) = \sqrt{(p_x - q_x)^2 + (p_y - q_y)^2}.$$

References

- [1] Training in echocardiography. Education and Training Subcommittee of the British Society of Echocardiography, *Br. Heart J.* 71 (1994) 2–5.
- [2] N. Evans, G. Malcolm, *Practical Echocardiography for the Neonatologist*, CD-ROM, Royal Prince Alfred Hospital, Sydney, Australia, 2001.
- [3] G.A. Mooney, J.G. Bligh, Information technology in medical education: current and future applications, *Postgrad. Med. J.* 73 (1997) 701–704.
- [4] M. Reznick, P. Harter, T. Krummel, Virtual reality and simulation: training the future emergency physician, *Acad. Emerg. Med.* 9 (2002) 78–87.
- [5] K. Tegtmeyer, L. Ibsen, B. Goldstein, Computer-assisted learning in critical care: from ENIAC to HAL, *Crit. Care Med.* 29 (2001) N177–N182.
- [6] T. Yambe, M. Yoshizawa, K. Tabayashi, H. Takeda, S. Nitta, Virtual percutaneous transluminal coronary angioplasty system for an educational support system, *Artif. Organs* 22 (1998) 710–713.
- [7] R. Ziegler, G. Fischer, W. Muller, M. Gobel, Virtual reality arthroscopy training simulator, *Comput. Biol. Med.* 25 (1995) 193–203.
- [8] S.L. Dawson, S. Cotin, D. Meglan, D.W. Shaffer, M.A. Ferrell, Designing a computer-based simulator for interventional cardiology training, *Catheter Cardiovasc. Interv.* 51 (2000) 522–527.
- [9] M. Blackwell, F. Morgan, A.M. DiGioia III, Augmented reality and its future in orthopaedics, *Clin. Orthop.* 354 (1998) 111–122.
- [10] S.L. Tang, C.K. Kwok, M.Y. Teo, N.W. Sing, K.V. Ling, Augmented reality systems for medical applications, *IEEE Eng. Med. Biol. Mag.* 17 (1998) 49–58.
- [11] D. Ost, A. DeRosiers, E.J. Britt, A.M. Fein, M.L. Lesser, A.C. Mehta, Assessment of a bronchoscopy simulator, *Am. J. Respir. Crit. Care Med.* 164 (2001) 2248–2255.
- [12] G. Meller, A typology of simulators for medical education, *J. Digit Imaging* 10 (1997) 194–196.
- [13] S.B. Issenberg, M.S. Gordon, D.L. Gordon, R.E. Safford, I.R. Hart, Simulation and new learning technologies, *Med. Teacher* 23 (2001) 16–23.
- [14] S. Pieper, M. Weidenbach, T. Berlage, Registration of 3D ultrasound images to surface models of the heart, in: *Proceedings of the Interfaces to Real & Virtual Worlds*, Montpellier, France, 1997, pp. 211–213.
- [15] M. Weidenbach, C. Wick, S. Pieper, K.J. Quast, T. Fox, G. Grunst, D.A. Redel, Augmented reality simulator for training in two-dimensional echocardiography, *Comput. Biomed. Res.* 33 (2000) 11–22.
- [16] M.E. Legget, D.F. Leotta, E.L. Bolson, J.A. McDonald, R.W. Martin, X.N. Li, C.M. Otto, F.H. Sheehan, System for quantitative three-dimensional echocardiography of the left ventricle based on a magnetic-field position and orientation sensing system, *IEEE Trans. Biomed. Eng.* 45 (1998) 494–504.
- [17] S. Trochim, *Situierendes Lernen in Augmented-Reality-basierten Trainingssystemen am Beispiel der Echokardiographie*, Doctoral Thesis, Verlag Dr. Hut, 2002.
- [18] M. Weidenbach, S. Pieper, S. Novak, C. Wick, T. Berlage, D.A. Redel, Evaluation of a landmark based registration for 3D echocardiographic data sets in an augmented reality application, in: F. Navarro-Lopez (Ed.), *Proceedings of the XXI Congress of the European Society of Cardiology*, Barcelona, Spain, 1999, pp. 931–935.
- [19] L.A. Zadeh, Fuzzy sets, *Inform. Control* 8 (1965) 338–353.
- [20] S. Kreutter, *Adaptive Hilfe in einem Trainingssystem für Echokardiographie*, Diploma Thesis, Friedrich-Alexander-Universität Erlangen, Nürnberg, 2001.
- [21] S.B. Issenberg, E.R. Petrusa, W.C. McGaghie, J.M. Felner, R.A. Waugh, I.S. Nash, I.R. Hart, Effectiveness of a computer-based system to teach bedside cardiology, *Acad. Med.* 74 (1999) S93–S95.

- [22] V. Chopra, B.J. Gesink, J. de Jong, J.G. Bovill, J. Spierdijk, R. Brand, Does training on an anaesthesia simulator lead to improvement in performance? *Br. J. Anaesth.* 73 (1994) 293–297.
- [23] E.R. Petrusa, S.B. Issenberg, J.W. Mayer, J.M. Felner, D.D. Brown, R.A. Waugh, G.T. Kondos, I.H. Gessner, W.C. McGaghie, Implementation of a four-year multimedia computer curriculum in cardiology at six medical schools, *Acad. Med.* 74 (1999) 123–129.
- [24] G. Gregoratos, A.B. Miller, 30th Bethesda conference: the future of academic cardiology. Task force 3: teaching, *J. Am. Coll. Cardiol.* 33 (1999) 1120–1127.
- [25] W.L. Henry, A. DeMaria, R. Gramiak, D.L. King, J.A. Kisslo, R.L. Popp, D.J. Sahn, N.B. Schiller, A. Tajik, L.E. Teichholz, A.E. Weyman, Report of the American Society of Echocardiography Committee on Nomenclature and Standards in Two-dimensional Echocardiography, *Circulation* 62 (1980) 212–217.
- [26] D.L. King, M.R. Harrison, D.L. King Jr., A.S. Gopal, O.L. Kwan, A.N. DeMaria, Ultrasound beam orientation during standard two-dimensional imaging: assessment by three-dimensional echocardiography, *J. Am. Soc. Echocardiogr.* 5 (1992) 569–576.
- [27] S. Trochim, M. Weidenbach, S. Pieper, C. Wick, T. Berlage, An enabling system for echocardiography providing adaptive support through behavioral analysis, *Stud. Health Technol. Inform.* 81 (2001) 528–533.
- [28] F.K. Klawonn, A. Keller, Fuzzy clustering based on modified distance measures, in: D.J. Hand, J.N. Kok, M.R. Berthold (Eds.), *IDA, Springer, Amsterdam, The Netherlands, 1999*, pp. 291–301.

Michael Weidenbach, MD, worked in the Department of Pediatric Cardiology at the University of Bonn when he joined an international research group at the Fraunhofer Institute for Applied Information Technology (FIT) focusing on Virtual Reality and Enabling technology. Currently he is working at the Department of Pediatric Cardiology, Heart Center at the University of Leipzig. His main interests are pediatric echocardiography and computer based medical training.

Sabine Trochim received her Ph.D. in Computer Science at the University of Bielefeld in 2002. In her doctoral dissertation, which she wrote at the Fraunhofer Institute for Applied Information Technology (FIT) she worked on the analysis of sensorimotor behavior to facilitate situated learning in medical training systems. Currently, she is employed at BioSolve IT, St. Augustin. Her main interests are methods of data analysis and machine learning and their application to biological and medical problems.

Steffan Kreutter studied Computer Science at the Friedrich-Alexander-University of Erlangen-Nuremberg and wrote his diploma thesis at the Fraunhofer Institute for Applied Information Technology (FIT), St. Augustin, Germany, where he worked on medical training systems. He is currently employed at the Fraunhofer Institute, FIT doing research and development on advanced data management and visualization tools for biological data.

Christian Richter, MD, is working in the Department of Pediatric cardiology at the University of Bonn. His main interest is pediatric echocardiography.

Thomas Berlage has studied computer science and received a Ph.D. from the University of Paderborn in 1993. His fields of work include object-oriented modelling, graphical user interfaces, enhanced reality and biomedical information systems. In 2002 he has been appointed as a professor at Aachen Technical University and as director at the Fraunhofer Institute for Applied Information Technology (FIT) in Sankt Augustin, where he is responsible for the research group Life Science Informatics.

Gernoth Grunst received his Ph.D. on linguistics at the Ruhr University Bochum in 1974. Currently, he is working at the Fraunhofer Institute for Applied Information Technology (FIT). His research interests are focusing on cognitive effects of multimedia and knowledge based orientation concepts. Since 1992 he has led several projects in the research group Life Science Informatics. The developments covered medical training, tele-cooperation, and navigation systems. Common feature has been the integration of medical 3-D image data with Virtual Reality elements into Augmented Reality scenarios.